

A Reliability-Based Assessment and Design Calibration of the Modified Strut-and-Tie Model for Steel Fiber Reinforced Concrete Deep Beams

Bac An Hoang

Ho Chi Minh City University of Architecture, Ho Chi Minh City, Vietnam
an.hoangbac@uah.edu.vn (corresponding author)

Quynh Nhu Nguyen-Thi

Ho Chi Minh City University of Architecture, Ho Chi Minh City, Vietnam
nhu.nguyenthiquynh@uah.edu.vn

Van Phuc Tran

Ho Chi Minh City University of Architecture, Ho Chi Minh City, Vietnam
phuc.tranvan@uah.edu.vn

Received: 28 September 2025 | Revised: 19 October 2025, 27 October 2025, and 30 October 2025 | Accepted: 1 November 2025

Licensed under a CC-BY 4.0 license | Copyright (c) by the authors | DOI: <https://doi.org/10.48084/etasr.15203>

ABSTRACT

A reliability analysis is performed on a modified Strut-and-Tie Model (STM), which accurately predicts the shear capacity of Steel Fiber Reinforced Concrete (SFRC) deep beams. However, inherent uncertainties are not considered when calculating the model's performance. This study implements a reliability analysis using Monte Carlo Simulation (MCS) on a dataset of 22 large-scale experimental samples, including samples with a simple supported and a two-span continuous configuration. In addition, a limit state function was established based on the modified STM model. Specifically, the analysis quantified the inherent safety of the uncalibrated model, revealing a reliability index (β) between 0.5 and 2.0. A reliability-based calibration was performed to address the issue of its composition not conforming with modern codes. For the Load and Resistance Factor Design (LRFD) format, a resistance factor (ϕ) of 0.50 was calculated, ensuring that different beam configurations achieve a consistent target reliability level.

Keywords-steel fiber reinforced concrete deep beams; strut-and-tie model; structural reliability; reliability-based calibration; resistance factor; Lfrd

I. INTRODUCTION

Deep beams are characterized by a large depth-to-span ratio and are critical structural elements in applications such as transfer girders and foundation walls [1]. The load transfer mechanism of deep beams has been effectively utilized by STM [2]. The same methodology was later adopted by ACI 318 and Eurocode 2 design codes [3, 4]. However, the accuracy of traditional STM approaches is limited by inherent simplifications. This challenge can be addressed by refined models, such as semi-empirical equations for deep beams with web openings or experimentally validated modifications for different structural members [5, 6].

SFRC is utilized to enhance structural performance. In [7], the inclusion of discrete steel fibers improves concrete's tensile strength, ductility, and crack control, making it an ideal

methodology for shear-dominant elements. Authors in [8] demonstrated that applying layers of fiber-reinforced polymer ultra-high-performance concrete composite layers enhances the shear capacity of existing deep beams. Authors in [9] revealed the superior shear behavior of SFRC deep beams. Authors in [10] focused on simply supported configurations with limited attention to the more complex continuous scenarios. A direct experimental comparison between Simple (SB) and Continuous (CB) SFRC deep beams was provided in [11].

A modified STM for SFRC deep beams was developed and experimentally validated in [12]. This model is selected for the current reliability-based investigation due to its on average high predictive accuracy and its relative simplicity. The probabilistic performance and inherent safety level of this model remain unquantified. In [13, 14], a framework for such evaluations was provided utilizing structural reliability analysis. The reliability-

based design optimization of composite beams, using MCS, was performed in [15]. General reliability assessments were conducted for STM in [16]. However, as proposed in [12], a formal, comprehensive reliability-based calibration of the specific modified STM has not yet been attempted. In the current codes, ϕ was calibrated for conventional concrete and standard models, not appropriate for this specific modified model and composite material.

Consequently, the present study performs a reliability-based assessment and calibration of the modified STM for SFRC deep beams. The primary objectives include: (a) establishing a robust limit state function for the model; (b) evaluating β for a diverse range of SFRC deep beam configurations; (c) analyzing the influence of key parameters on the reliability level; (d) calibrating ϕ for the LRFD format. The results will provide valuable insights into the actual safety levels of the modified STM and contribute to the development of a more efficient and probabilistically consistent design tool for practicing engineers.

II. METHODOLOGY

Four main steps are involved in conducting the reliability-based assessment and calibration, as illustrated in Figure 1.

A. Limit State Function

A limit state function ($g(X)$) governs the reliability analysis, which defines the boundary between the safe and

failure states. It is formulated as the difference between the structure's resistance (R) and the applied load effect (S), calculated by:

$$g(X) = R - S \tag{1}$$

where X is the vector of all random variables. Failure is presumed to occur if $g(X) \leq 0$. The R is expressed as the product of the nominal capacity (V_n) predicted by the model and a model uncertainty factor (M), as shown in:

$$R = M \cdot V_n \tag{2}$$

The V_n is determined by the governing failure mode from the modified STM, which enhances the traditional ACI 318 framework, with two empirical adjustments derived from [12].

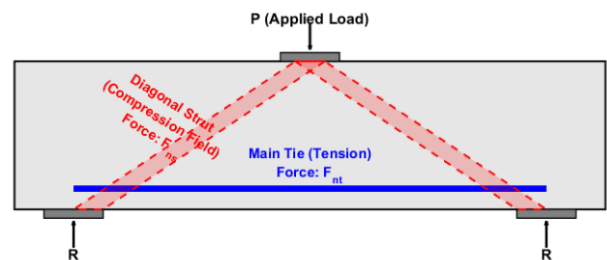


Fig. 1. STM idealization for a deep beam.

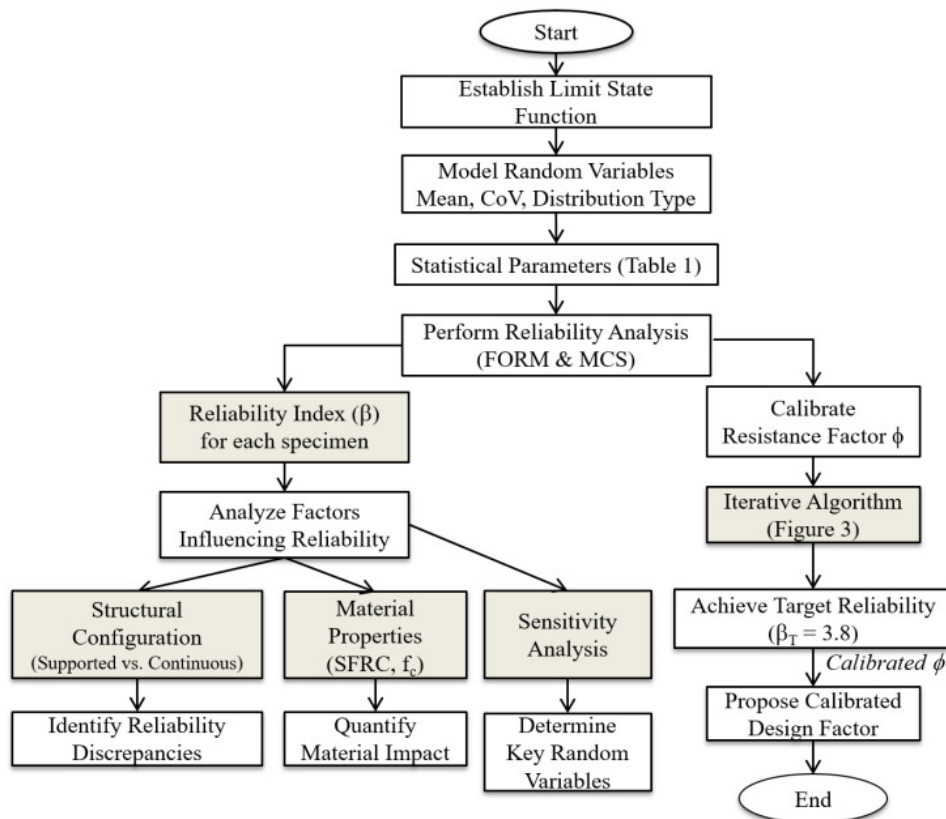


Fig. 2. Methodology flowchart of the study.

In the standard ACI 318 model, the V_n of a compression strut is given by:

$$F_{ns} = f_{ce} \cdot A_{cs} \quad (3)$$

where f_{ce} is the effective compressive strength of the concrete in the strut. First, the capacity of the compression strut (F_{ns}) is calculated using a novel strengthening factor (α) which replaces the standard ACI 318 strut effectiveness factor (β_s), as presented in:

$$F_{ns} = \alpha(0.85\beta_s f'_c)A_{cs} \quad (4)$$

where f'_c is the concrete compressive strength, A_{cs} is the cross-sectional area of the strut. α is calibrated from experimental data, as depicted in (5). While β_s accounts for confinement from conventional stirrups, the proposed α factor is an empirical formulation designed to capture the combined, synergistic confinement effect of both steel fibers and transverse stirrups in SFRC deep beams:

$$\alpha = 0.3V_f + 1.5\rho_{sw} + 1.4 \quad (5)$$

where V_f is the steel fiber volume fraction and ρ_{sw} is the stirrup ratio. The capacity of the tension tie (F_{nt}), calculated by (6), is adjusted by a reduction factor (γ) to reflect the experimental observation that the longitudinal reinforcement does not reach its full yield strength at ultimate shear failure [12]:

$$F_{nt} = \gamma(A_s f_y) \quad (6)$$

where A_s is the area of the longitudinal reinforcement, (f_y) is the yield strength of the reinforcement, and γ is set to 0.88 for

SB and to 0.86 for C.B. beams. These values are determined as the average measured ratio of the maximum reinforcement strain at ultimate load to the steel's yield strain, calculated from the experimental data for each beam configuration. The S , presented in (7), is the sum of the unfactored dead load (D) and live load (L), with both of them treated as random variables:

$$S = D + L \quad (7)$$

Finally, the limit state function used for the reliability analysis is presented in:

$$g(X) = M \cdot V_n(X_R) - (D + L) \quad (8)$$

where $V_n(X_R)$ represents the nominal shear capacity as a function of the vector of resistance variables (X_R).

B. Random Variable Modeling

To account for the inherent uncertainties in the analysis, parameters influencing both resistance and load were modeled as random variables. The statistical properties of these variables, including their mean (μ), coefficient of variation (CoV), and probability distribution type, are summarized in Table I. These parameters were established based on experimental data from [12]. They were also supplemented with recommendations from established sources such as the JCSS Probabilistic Model Code and other reliability literature [3, 13, 16]. An expanded database was utilized to statistically characterize M through an expanded database of 37 relevant SFRC deep beam tests [11, 17-19]. The load uncertainties reflect standard assumptions used in LRFD calibration [14].

TABLE I. STATISTICAL PARAMETERS OF RANDOM VARIABLES

Uncertainty category	Variable	μ	CoV	Dist. Type	Comments / reference
Material	f'_c	43.1 MPa and 58.1 MPa	0.10 - 0.15	Lognormal	Mean from tests [12]; $CoV/dist.$ from literature [14, 17]
	f_y	508 - 516 MPa	0.05	Lognormal	
	Yield Strength of Stirrups (f_{yv})	317 MPa	0.05	Lognormal	
Geometric	Beam Height (h)	500 mm	0.03	Normal	Construction tolerance [17]
	Beam Width (b)	150 mm	0.05	Normal	
Model	M	1.04	0.20	Lognormal	From 37-beam database [12, 18, 20]
Load	D	Nominal	0.10	Normal	Standard LRFD assumptions [14]
	L	Nominal	0.25	Gumbel	

C. Reliability Analysis Methods

In structural reliability analysis, the methods available to evaluate the probability of failure are categorized into analytical methods, such as the First-Order Reliability Methods (FORM) and Second-Order Reliability Methods (SORM), and simulation-based methods, such as MCS. Highly non-linear limit state functions or non-normal random variables can compromise the accuracy of analytical methods. MCS was chosen as the primary analysis method in this study to address these limitations. MCS is an efficient numerical technique, particularly well-suited for complex and non-linear limit state functions. In this approach, the probability of failure (P_f) was estimated by generating two million random sample sets for all input variables according to their defined probability distributions and counting the instances of failure (where

$g(X) \leq 0$) [13]. The β index was then derived using the inverse standard normal cumulative distribution function, presented in:

$$\beta = \Phi^{-1}(1 - P_f) \quad (9)$$

The analytical FORM was employed for verification. This method linearizes the limit state function at the most probable point of failure and approximates β as shown in:

$$\beta \approx \frac{\mu_g}{\sigma_g} \quad (10)$$

where μ_g and σ_g are the mean and standard deviation of the limit state function, respectively.

D. Resistance Factor Reliability-Based Calibration

The final objective is to calibrate a ϕ value for the modified STM. This calibration is performed to be compatible with the LRFD format presented in modern codes. The LRFD principle requires that the factored resistance meets or exceeds the factored load effects, as indicated by:

$$\phi R_n \geq \gamma_D D + \gamma_L L \tag{11}$$

The optimal ϕ value of the calibration process ensures a consistent target reliability index (β_T) across different designs. Based on ACI 318 recommendations for shear-critical components, a target of β_T with a 3.8 value is adopted [3]. The calibration uses ASCE 7 load factors ($\gamma_D=1.2, \gamma_L=1.6$), whose probabilistic basis was established in [21]. In addition, these factors are maintained in current design standards, such as those provided in [22], and assume a nominal live-to-dead (L/D) ratio of 0.5.

An iterative algorithm, represented in Figure 3, is employed to determine the optimal ϕ .

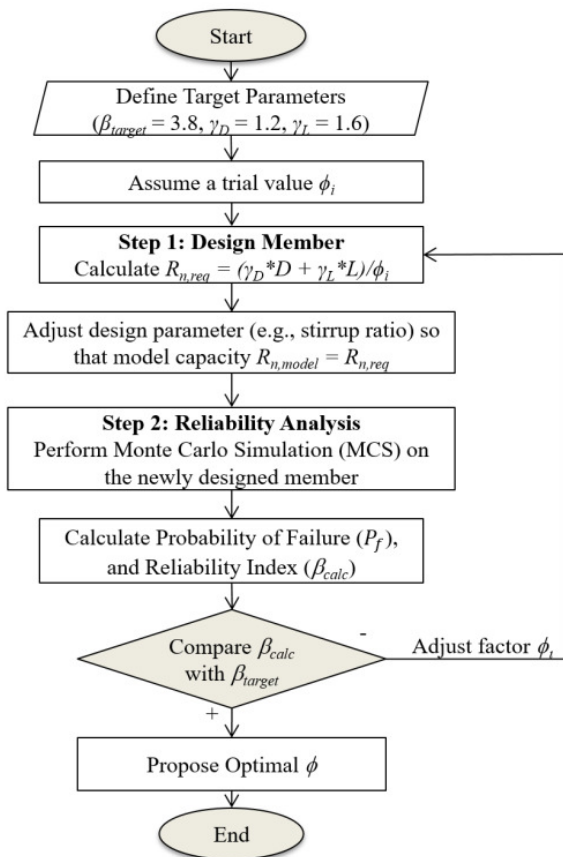


Fig. 3. Iterative algorithm for resistance factor calibration.

This algorithm details the "Calibrate Resistance Factor" step, outlined in Figure 1. The optimal value of ϕ minimizes the objective function, defined as the sum of squared differences between the calculated β for each of the k design cases (β_i) and the β_T , as described by:

$$\text{minimize } f(\phi) = \sum_{i=1}^k (\beta_i - \beta_T)^2 \tag{12}$$

The algorithm begins with a trial ϕ . For each design case, the required nominal resistance ($R_{n,req}$) is determined from (11), and a key design parameter is adjusted until the model's predicted capacity matches $R_{n,req}$. A reliability analysis is then performed on this final design to compute its β_i . The process is repeated with adjusted ϕ values until the error in (12) is minimized. This minimization problem was solved numerically by iteratively testing a range of ϕ values and selecting the value that resulted in the lowest sum of squared errors.

This iterative calibration process ensures that the proposed ϕ provides a consistent and appropriate level of safety for SFRC deep beams designed using the modified STM, reflecting the probabilistic nature of both resistance and load uncertainties.

III. RESULTS AND DISCUSSION

A. Uncalibrated Model Reliability for Case Study Specimens

The reliability assessment of this study utilizes a dataset of 22 large-scale deep beam specimens from the foundational research project RD 34-22 [12]. Parameters, including structural configuration (simple supported and two-span continuous), f'_c (43.1 MPa and 58.1 MPa), steel fiber content (0, 30, and 45 kg/m³), and ρ_{sw} (0.15% and 0.30%) were calculated. Figures 4 and 5 schematically illustrate the setup for SB and CB, respectively.

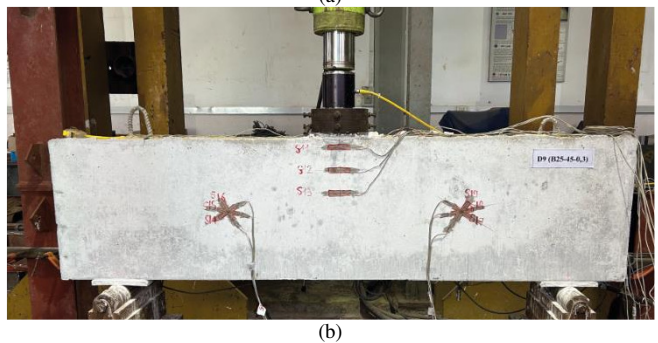
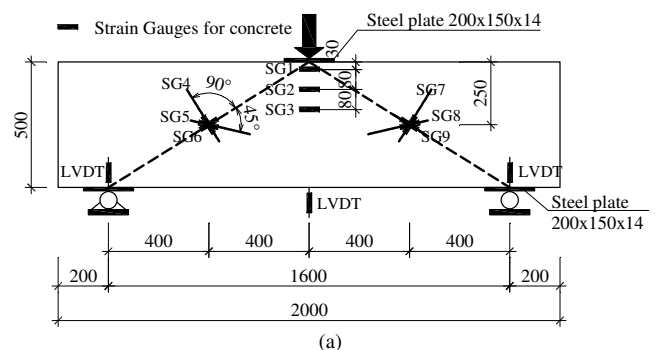
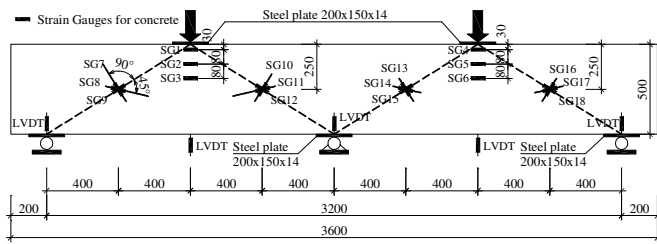
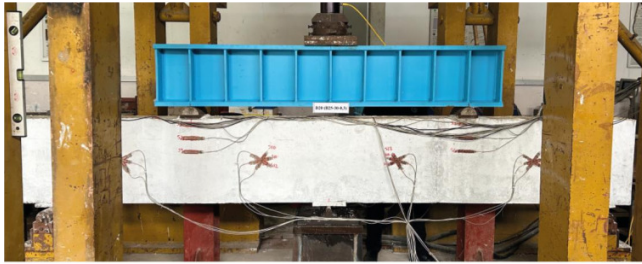


Fig. 4. (a) Schematic representation and (b) actual setup of an SB.



(a)



(b)

Fig. 5. (a) Schematic representation and (b) actual setup of a CB.

M was calibrated using a heterogeneous database of 37 specimens, derived from 37 simply supported SFRC deep beams, although the core dataset of 22 specimens indicated consistency for the primary analysis. The expanded dataset utilized for the calibrations is detailed in Table II, summarizing the range of key parameters of this database, and thus confirming its comprehensive and heterogeneous nature.

TABLE II. PARAMETER RANGES OF THE 37-BEAM DATABASE

Ref.	No. of beams	a/d ratio	f'_c (MPa)	V_f (%)	ρ_{sw} (%)
[12]	6	1.8	34.5 - 38.4	0.0 - 0.6	0.15 - 0.30
[17]	9	1.5	29.4 - 32.3	0.0 - 1.0	0.00 - 0.30
[18]	5	0.9	56.2 - 61.1	0.0 - 2.0	0.00 - 0.70
[20]	17	1.8	25.4 - 35.0	0.0 - 0.8	0.10 - 0.30

The key properties, experimental results, and reliability analysis outcomes for all specimens are summarized in Table III. The analysis demonstrates that the uncalibrated modified STM yields low and inconsistent safety levels, with calculated β ranging between 0.53 and 1.99. This range is significantly below the required β_T for shear-critical elements [3, 20]. The low β indices, calculated for the non-fibrous control beams, do not invalidate the ACI 318 STM. In contrast, they indicate that the specific empirical factors (α and γ) of the modified STM require a formal calibration to ensure a consistent target safety level across its entire intended range of application, from non-fibrous to fiber-reinforced concrete. V_f is calculated assuming a steel fiber density of 7850 kg/m^3 , while Δ is calculated by:

$$\Delta = \frac{\beta_{MCS} - \beta_{FORM}}{\beta_{MCS}} \quad (13)$$

Figure 6 illustrates a consistent discrepancy between the MCS and the verification FORM results, with FORM yielding β values between 23% and 35% lower.

TABLE III. SUMMARY OF SPECIMEN PROPERTIES, EXPERIMENTAL RESULTS, AND RELIABILITY INDICES

Specimen ID	Configuration	f'_c (MPa)	m_f (kg/m ³)	V_f (%)	ρ_{sw} (%)	$P_{u,exp}$ (kN)	β_{MCS}	β_{FORM}	Δ (%)
S-40-00-0,15	SB	43.1	0	0	0.15	540	0.97	0.73	24.9
S-40-30-0,15	SB	43.1	30	0.38	0.15	580	0.96	0.71	25.8
S-40-45-0,15	SB	43.1	45	0.57	0.15	660	0.61	0.42	32.1
S-40-00-0,30	SB	43.1	0	0	0.30	680	0.61	0.42	32.0
S-40-30-0,30	SB	43.1	30	0.38	0.30	720	0.62	0.42	31.9
S-40-45-0,30	SB	43.1	45	0.57	0.30	760	0.53	0.34	35.4
S-50-00-0,15	SB	58.1	0	0	0.15	560	1.93	1.45	25.1
S-50-30-0,15	SB	58.1	30	0.38	0.15	620	1.80	1.35	25.0
S-50-45-0,15	SB	58.1	45	0.57	0.15	700	1.48	1.12	24.6
S-50-00-0,30	SB	58.1	0	0	0.30	720	1.49	1.14	23.6
S-50-30-0,30	SB	58.1	30	0.38	0.30	780	1.41	1.08	23.4
S-50-45-0,30	SB	58.1	45	0.57	0.30	820	1.33	1.03	23.0
C-40-00-0,15	CB	43.1	0	0	0.15	540	0.97	0.73	24.9
C-40-30-0,15	CB	43.1	30	0.38	0.15	550	1.16	0.88	23.8
C-40-45-0,15	CB	43.1	45	0.57	0.15	610	0.90	0.66	26.0
C-40-00-0,30	CB	43.1	0	0	0.30	610	1.00	0.75	25.0
C-40-30-0,30	CB	43.1	30	0.38	0.30	650	0.99	0.75	25.0
C-50-00-0,15	CB	58.1	0	0	0.15	560	1.93	1.43	25.8
C-50-30-0,15	CB	58.1	30	0.38	0.15	590	1.99	1.47	26.2
C-50-45-0,15	CB	58.1	45	0.57	0.15	640	1.81	1.36	24.7
C-50-00-0,30	CB	58.1	0	0	0.30	650	1.86	1.39	25.1
C-50-30-0,30	CB	58.1	30	0.38	0.30	710	1.76	1.32	25.0

This difference is attributed to the high non-linearity of the limit state function and the presence of non-normal random variables [12, 13]. Therefore, MCS is considered the more efficient benchmark for this study.

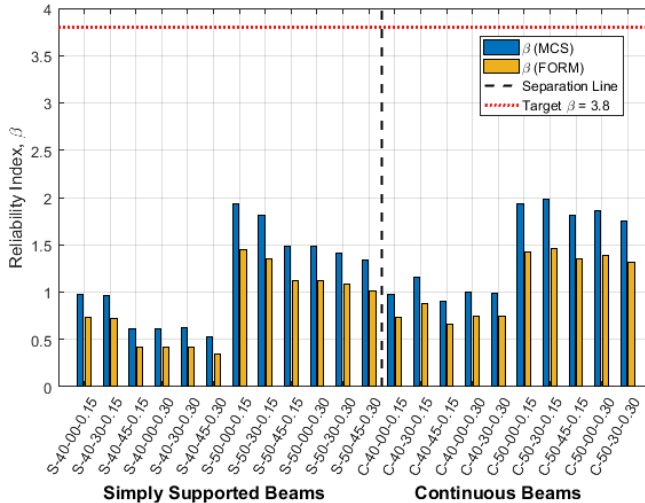


Fig. 6. Comparison of β from MCS and FORM.

These findings demonstrate that the uncalibrated model is not suitable for direct design, highlighting the necessity of a formal reliability-based calibration for adequate and uniform safety.

B. Analysis of Factors Influencing Reliability

The low and inconsistent β values are a direct consequence of the predictive model's characteristics rather than the beams' physical performance. A critical and counterintuitive trend was observed, where increasing the amount of shear reinforcement led to a decrease in the calculated β index. For instance, in SB with 58.1 MPa concrete, increasing the steel fiber content from 0 to 45 kg/m³ led to a decrease of β_{MCS} from 1.49 to 1.33. This result can be attributed to the model's sensitivity. Adding reinforcement leads to a physically stronger beam. This performance enhancement is not proportionally captured by the modified STM's formula. Consequently, the analytical safety margin (μ_R/μ_S) decreases for more heavily reinforced beams, resulting in a lower calculated β .

The observed trend indicates that while the modified STM provides a safe lower-bound prediction, its formulation becomes progressively more conservative for more heavily reinforced sections. The model underestimates the performance gains provided by higher quantities of steel fibers and stirrups. Consequently, for designs with high reinforcement ratios, the actual safety margin is much higher than the one suggested by the calculated β . This ensures a safe design, but leads to a less cost-effective option.

C. Concrete Strength and Beam Configuration Influence

Increasing f'_c consistently led to a significant increase in β . For example, for two beams with 45 kg/m³ of fibers and a ρ_{sw} equal to 0.30%, increasing f'_c from 43.1 MPa to 58.1 MPa led to an increase in β_{MCS} from 0.53 to 1.33. This confirms that

the model is appropriately sensitive to this primary parameter. A more detailed experimental analysis focusing specifically on the effect of f'_c on the shear behavior and fiber efficiency for two of these beams is provided in [23]. In this assessment, S was set equal to the experimentally measured ultimate capacity ($P_{u,exp}$). The experimental results indicated that CB failed at a lower ultimate load than their SB, analyzed with a lower S . Consequently, a larger analytical safety margin ($R - S$) was observed along with a slightly higher calculated β . The strengthening effect of steel fibers tends to be less pronounced in continuous configurations [11].

D. Dominant Random Variables

The sensitivity analysis was performed using a variance-based method. The squared Spearman rank correlation coefficients between each random input variable and the limit state function output were calculated from the MCS samples. These coefficients were then normalized to sum to 100%, representing the percentage contribution of each variable's uncertainty to the total output variance. A sensitivity analysis was performed to quantify the contribution of each random variable to the total variance of the limit state function. The results, as illustrated for a representative specimen in Table IV and Figure 7, consistently indicate that the M and f'_c are the two dominant factors. Together, they contribute to over 85% of the total variance, 55.846% from M and 30.997% from f'_c , respectively.

TABLE IV. SENSITIVITY ANALYSIS RESULTS

Variable	Contribution
M	0.55846
f'_c	0.30997
LL	0.04733
b	0.03414
DL	0.03349
h	0.01658

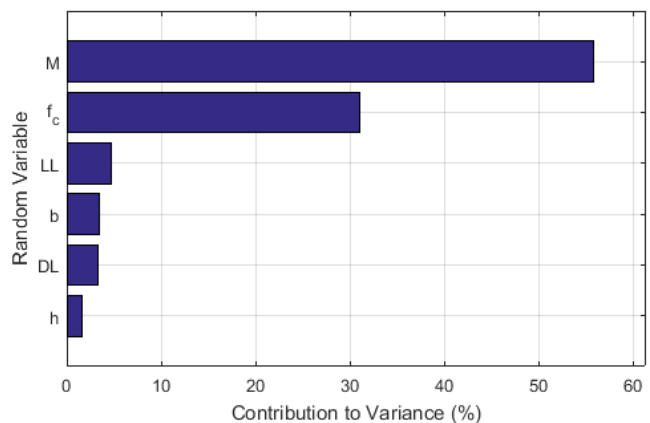


Fig. 7. Sensitivity analysis for a representative specimen.

E. Resistance Factor Calibration

The uncalibrated model yields inadequate safety levels, thus necessitating a reliability-based calibration to ensure that designs achieve a consistent β_T . To achieve this, a ϕ was calibrated for the entire dataset of 22 beam specimens. A

sensitivity analysis was first performed for various L/D, with the results summarized in Table V. The optimal ϕ was found to vary moderately with the load composition, increasing from 0.50 for dead-load dominant scenarios to 0.60 for live-load dominant scenarios (L/D = 2.0).

TABLE V. INFLUENCE OF L/D RATIO ON CALIBRATED RESISTANCE FACTOR

L/D ratio	Optimal calibrated ϕ	Average achieved β
0.25	0.50	3.671
0.5	0.50	3.902
1.0	0.55	3.789
2.0	0.6	3.649

To ensure a safe design across a wide range of conditions, a single, conservative of ϕ equal to 0.50 is proposed. This relatively low ϕ value is a direct consequence of the high model uncertainty (CoV = 0.20), which the sensitivity analysis confirmed as the dominant variable. This level of variability, while within the typical range of 0.15-0.25 reported in other probabilistic studies for SFRC shear models, stems from the model's inherent simplifications in capturing the complex, non-linear interactions between steel fibers, stirrups, and concrete confinement. Therefore, the conservative ϕ is not an arbitrary choice but a quantitatively justified measure to counteract the model's predictive variability. A critical direction for future research should be the refinement of the predictive model itself, as an improved formulation with lower uncertainty could justify a higher, more economically efficient resistance factor.

IV. CONCLUSIONS

This study performed a comprehensive reliability-based assessment and calibration of a modified Strut-and-Tie Model (STM) for Steel Fiber Reinforced Concrete (SFRC) deep beams. Based on the results, the following conclusions are drawn in alignment with the research objectives:

1. A robust limit state function was successfully established for the modified STM. This function explicitly incorporated the inherent uncertainties in material properties, geometric dimensions, the predictive model itself, and applied loads, providing a sound basis for the subsequent reliability analysis.
2. The reliability of the uncalibrated model was evaluated, revealing low and inconsistent safety levels. The calculated reliability indices (β) for the as-built experimental beams ranged from 0.53 to 1.99, demonstrating that they were significantly lower than the target value of 3.8 required by modern design codes and underscoring the necessity of a formal calibration.
3. The influence of key parameters on reliability was analyzed. The analysis clarified that the low β values stemmed from a limitation in the model's sensitivity, which underestimates performance gains in stronger beams. Furthermore, a sensitivity analysis identified that model uncertainty (M) and concrete compressive strength (f'_c)

were the two most dominant variables, together contributing over 85% of the total variance.

4. A resistance factor (ϕ) was calibrated for the Load and Resistance Factor Design (LRFD) format. Based on an iterative process targeting a consistent safety level, a resistance factor of $\phi = 0.50$ is proposed. This value, while conservative, is a direct, quantitatively derived consequence of the high model uncertainty (CoV = 0.20) and is essential to ensure that SFRC deep beams designed with this modified STM consistently achieve the required high level of safety.

Finally, it is acknowledged that ϕ was calibrated using a specific dataset. Future research should, therefore, focus on several key areas: (1) refining the formulation of α to develop a non-linear model that more accurately captures the dose-dependent effect of reinforcement; (2) extending the reliability analysis to consider other potential failure modes, such as nodal zone crushing; and (3) validating the proposed ϕ -factor against a wider, more diverse database of experiments from independent researchers to establish its general applicability and robustness.

REFERENCES

- [1] N. Zhang and K.-H. Tan, "Direct Strut-and-Tie Model for Single Span and Continuous Deep Beams," *Engineering Structures*, vol. 29, no. 11, pp. 2987–3001, Nov. 2007, <https://doi.org/10.1016/j.engstruct.2007.02.004>.
- [2] J. Schlaich and K. Schäfer, "Zur Druck-Querkraft-Festigkeit des Stahlbetons," *Beton- und Stahlbetonbau*, vol. 78, no. 3, pp. 73–78, 1983, <https://doi.org/10.1002/best.198300120>.
- [3] *Building Code Requirements for Structural Concrete and Commentary*, ACI 318-19, American Concrete Institute, Farmington Hills, MI, USA, 2019.
- [4] *Design of Concrete Structures. Part 1.1: General Rules and Rules for Buildings*, EN 1992-1-1, European Committee for Standardization, Brussels, Belgium, 2004.
- [5] L. T. Hussein and R. M. Abbas, "A Semi-Empirical Equation based on the Strut-and-Tie Model for the Shear Strength Prediction of Deep Beams with Multiple Large Web Openings," *Engineering, Technology & Applied Science Research*, vol. 12, no. 2, pp. 8289–8295, Apr. 2022, <https://doi.org/10.48084/etasr.4743>.
- [6] A. Starčev-Čurčin *et al.*, "Experimental Testing of Reinforced Concrete Deep Beams Designed by Strut-And-Tie Method," *Applied Sciences*, vol. 10, no. 18, Sept. 2020, <https://doi.org/10.3390/app10186217>.
- [7] A. Ali, Z. Soomro, S. Iqbal, N. Bhatti, and A. F. Abro, "Comparison of Mechanical Properties of Lightweight and Normal Weight Concretes Reinforced with Steel Fibers," *Engineering, Technology & Applied Science Research*, vol. 8, no. 2, pp. 2741–2744, Apr. 2018, <https://doi.org/10.48084/etasr.1874>.
- [8] K.-F. Weng, J.-X. Zhu, B.-T. Huang, J.-G. Dai, and J.-F. Chen, "Shear strengthening of reinforced concrete beams using FRP-UHPC composite layer," *Composite Structures*, Dec. 2025, Art. no. 119931, <https://doi.org/10.1016/j.compstruct.2025.119931>.
- [9] A. M. Yousef, A. M. Tahwia, M. S. Al-Enezi, A. M. Yousef, A. M. Tahwia, and M. S. Al-Enezi, "Experimental and Numerical Study of UHPFRC Continuous Deep Beams with Openings," *Buildings*, vol. 13, no. 7, July 2023, <https://doi.org/10.3390/buildings13071723>.
- [10] M. Deng, F. Ma, X. Wang, and H. Lü, "Investigation on the shear behavior of steel reinforced NC/HDC continuous deep beam," *Structures*, vol. 23, pp. 20–25, Feb. 2020, <https://doi.org/10.1016/j.istruc.2019.10.002>.
- [11] N. T. Q. Nhu, T. N. L. Tuyen, N. M. Long, H. B. An, P. T. Le, and T. V. Phuc, "Phân tích thực nghiệm ứng xử cắt của dầm cao bê tông sợi thép

- liên tục và đơn giản." *Tạp chí Khoa học Công nghệ Xây dựng (TCKHCN XD) - ĐHXDHN*, vol. 19, no. 2V, pp. 28–41, May 2025, [https://doi.org/10.31814/stce.huce2025-19\(2V\)-03](https://doi.org/10.31814/stce.huce2025-19(2V)-03).
- [12] *Research on the Bearing Capacity and Deformation of Transfer Beam Structures for High-Rise Buildings Using High-Strength Concrete and High-Strength Concrete Reinforced With Dispersed Steel Fibers*, RD 34-22, Ministry of Science and Technology, Ho Minh City, Vietnam, 2024.
- [13] R. E. Melchers and A. T. Beck, *Structural Reliability Analysis and Prediction*. New York, NY, USA: John Wiley & Sons, 2018.
- [14] A. S. Nowak and K. R. Collins, *Reliability of Structures, Second Edition*. Boca Raton, FL, USA: CRC Press, 2012.
- [15] T. H. Nguyen, V. D. Le, X. H. Vu, and D. K. Nguyen, "Reliability-based Design Optimization of Steel-Concrete Composite Beams Using Genetic Algorithm and Monte Carlo Simulation," *Engineering, Technology & Applied Science Research*, vol. 12, no. 6, pp. 9766–9770, Dec. 2022, <https://doi.org/10.48084/etasr.5366>.
- [16] D. Muendacha, J. Teerawong, and P. Chetchotisak, "A Safety-Based Evaluation of Strut-and-Tie Methods for Shear Design of RC Deep Beams in Accordance With International Concrete Codes," *Engineering and Applied Science Research*, vol. 47, no. 2, pp. 137–144, June 2020.
- [17] *Probabilistic Model Code*, JCSS, Joint Committee on Structural Safety, Zürich, Switzerland, 2006.
- [18] R. G. Tuchscherer and A. Quesada, "Replacement of Deformed Side-Face Steel Reinforcement in Deep Beams With Steel Fibers," *Structures*, vol. 3, pp. 130–136, Aug. 2015, <https://doi.org/10.1016/j.istruc.2015.03.008>.
- [19] K. Ma *et al.*, "Shear Behavior of Hybrid Fiber Reinforced Concrete Deep Beams," *Materials*, vol. 11, no. 10, Oct. 2018, <https://doi.org/10.3390/ma11102023>.
- [20] T. D. Dang, D. T. Tran, L. Nguyen-Minh, and A. Y. Nassif, "Shear resistant capacity of steel fibres reinforced concrete deep beams: An experimental investigation and a new prediction model," *Structures*, vol. 33, pp. 2284–2300, Oct. 2021, <https://doi.org/10.1016/j.istruc.2021.05.091>.
- [21] *Development of a probability based load criterion for American National Standard A58*, National Institute of Standards and Technology, Gaithersburg, MD, USA, 1980.
- [22] *Minimum Design Loads and Associated Criteria for Buildings and Other Structures*, ASCE/SEI 7-22, American Society of Civil Engineers, Reston, VA, USA, 2022.
- [23] N. T. Q. Nhu, T. N. L. Tuyen, N. M. Long, H. B. An, P. T. Le, and T. V. Phuc, "Ảnh hưởng của cường độ bê tông đến ứng xử cắt của dầm cao bê tông sợi thép," *Tạp chí Khoa học Công nghệ Xây dựng (TCKHCN XD) - ĐHXDHN*, vol. 19, no. 3V, pp. 1–12, Aug. 2025, [https://doi.org/10.31814/stce.huce2025-19\(3V\)-01](https://doi.org/10.31814/stce.huce2025-19(3V)-01).